PHYSICAL REVIEW D VOLUME 20, NUMBER 4 15 AUGUST 1979

Diagrammatic approach to pair production in slowly varying and constant fields

C. B. Chiu*
Max-Planck-Institut für Physik und Astrophysik, München, Federal Republic of Germany
and University of Texas, Austin, Texas 78712

S. Nussinov†
Tel-Aviv University, Ramat-Aviv, Tel-Aviv, Israel
and Max-Planck-Institut für Physik und Astrophysik, München, Federal Republic of Germany

(Received 29 November 1978)

We consider the problem of pair creation in slowly varying and essentially constant fields using directly momentum-space Feynman diagrams for the pair production amplitude. When the production occurs via many interactions with small energy transfer, the problem can be viewed as an integration on paths in energy space. An estimate via the integral over the optimal path given by Hamilton's principle, a fuller Lagrangian equation, is introduced and discussed. The existence of such a classical path reflects in an asymptotic behavior such as $n!c^n$ of high-order Feynman diagrams, which in a formal Borel-type summation yields the essentially singular tunneling behavior in constant fields.

I. INTRODUCTION

The problems of charged-particle motion in constant, plane-wave, and space-constant, but time-periodic, electric (and magnetic) fields have been solved exactly.[1] In particular, these solutions were used to deduce the rate of electron- (with mass m and coupling g) positron pair creation

$$\frac{P}{VT}=(g\mathcal{E})^2\left[\exp\left(-\frac{\pi m^2}{g\mathcal{E}}\right)+\sum_{n=2}^{\infty}\exp\left(-\frac{n\pi m^2}{g\mathcal{E}}\right)\frac{1}{n^2}\right], \tag{1}$$

in a constant field $\mathcal{E}$.[2]

It is conceivable that a quantum-chromodynamic (QCD) analog of Eq. (1) may be relevant for multihadron production.[3] On the more theoretical side the exact solutions can find application in connection with the large-order behavior of (field-theory) perturbation series.[4] Previous approaches to the problem involve the equation of motion in configuration space where operator techniques could be used to reduce—the constant-$\mathcal{E}$ problem say—to harmonic motion.

In the following we address the general problem of pair creation in a slowly switched-on and -off field using the essentially different technique of direct study of momentum-space Feynman diagrams. The problem of finding the most likely path (in every space) via which a negative-energy particle $(-E,\vec{p})$ "moves" (due to many small energy transfers ω_i) to become the positive-energy particle $(E,\vec{p})$ is solved by classical-mechanics Lagrangian methods.

Two types of field-switching procedures should be clearly distinguished:

(a) There is a real precribed slow-switching-on procedure which generates real photons with a fixed and small average energy ω.

(b) The switching on and off is a formal device which allows us to approach the singular limit of "constant fields," since in strictly constant fields no nonzero frequencies exist and real pair creation vanishes identically to any finite order in perturbation theory.

In case (b) we have to make the frequency spread of the field Δ_n, used for nth-order diagram estimates, vanish like $1/n$. The pair-production diagrams have then the characteristic behavior

$$A_n\sim n!\,c^n\left(\frac{g\mathcal{E}}{m^2}\right)^n, \tag{2}$$

where c is proportional to the action integral of the energy-space Lagrangian and a formal Borel sum[5] yields

$$A=\sum_n A_n\sim\exp(-cm^2/g\mathcal{E}), \tag{3}$$

with the correct feature of the essentially nonperturbative tunneling-type behavior.

In general, pairs may emerge from both sources, owing to (a) real radiation converting into pairs and (b) tunneling.

The plan of this paper is as follows. In the next section we describe the nth-order diagrams and in Sec. III the optimal path (Lagrangian) approach to large-order diagrams. An exact [for case (b)] recipe involving quadratures only is given. Special cases of interest are then treated in various approximation in Sec. IV and, finally, we speculate on the possible applications of the method introduced.

II. THE nth-ORDER DIAGRAM FOR PAIR CREATION

For simplicity let us consider production of a pair of charged scalar particles.

The four-vector potential representing an $\vec{E}$ field along the three axes will be chosen as

$$A_\mu = (0, 0, 0, A_z = a(t)),\qquad E_3(t) = \frac{\partial a}{\partial t}. \tag{4}$$

The interaction of a scalar particle with A_μ is

$$V = -2g p_z a(t) + g^2 a^2(t), \tag{5}$$

or in momentum space

$$V = -2g p_z \tilde{a}(\omega)\delta^3(\vec{k}) + g^2\tilde{a}^2(\omega)\delta^3(\vec{k}), \tag{6}$$

where $\tilde{f}(\omega)$ is used for Fourier transforms. The pair-production diagram is indicated in Fig. 1. It represents scattering from a negative-energy state $(-E, \vec{p})$ to $(E, \vec{p})$ via n interactions with the field. At each such interaction a negative or positive energy ω_i is transferred. Since the ω_i are taken from narrow distributions $[\tilde{a}(\omega)$ or $\tilde{a}^2(\omega)]$ many such transfers with $\sum \omega_i = 2E$ are needed for on-shell $(p^2 + m^2 = E^2)$ pair creation. The propagator structure of the diagram is rather simple:

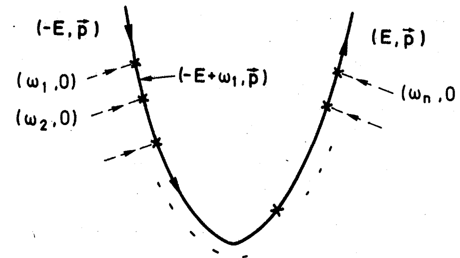

FIG. 1. A pair-production diagram.

$$D^{(n)} = (-1)^{n-1}\prod_{k=1}^{n-1}\left(2E - \sum_1^k \omega_i\right)\left(\sum_1^k \omega_i\right). \tag{7}$$

If, furthermore, we choose $p_z = 0$, i.e., $\vec{p} = (\vec{p}_T, 0)$ then $\vec{p}\cdot\vec{A} = 0$ and only the seagull term is maintained. In this case we have exactly one diagram in *each* even order of perturbation:

$$A_n = -(-g^2)^n \int \frac{\prod_{i=1}^n d\omega_i\,\tilde{a}^2(\omega_i)}{\prod_{k=1}^{n-1}\left(2E - \sum_i^k \omega_i\right)\sum_i^k \omega_i} \times \delta\left(\sum_i \omega_i - 2E\right). \tag{8}$$

In general for $p_z \neq 0$,

$$A_n = g^{2n}\sum_k A_{k,2n-2k},$$
$$A_{k,2n-2k} = (-2p_z)^{2n-2k}\int \prod_{i=1}^{2n-k} d\omega_i \sum_{\text{perm}} \tilde{a}^2(\omega_{i1})\cdots\tilde{a}^2(\omega_{ik})\tilde{a}^2(\omega_{j1})\cdots\tilde{a}^2(\omega_{j2n-2k})\,\frac{\delta(\sum\omega_i - 2E)}{D^{(2n-k)}}, \tag{9}$$

where the summation goes over the $\binom{2n-k}{k}$ ways of distributing k seagull vertices.

III. THE OPTIMAL-PATH (LAGRANGIAN) METHOD FOR ESTIMATING A_n

Let us denote $\sum_1^k \omega_i = q_k$. Focusing first on Eq. (8) we can view it as an integration over all possible paths describing the evolution of $q(k)$ from $q(0) = 0$ to $q(n) = 2E$ (Fig. 2). The weight W_{path} associated with each path consists of a product of two terms:

$$W_{\text{path}} = -(-g^2)^n w_1 w_2,$$
$$w_1 = \prod_k [q_k(2E - q_k)]^{-1}, \tag{10}$$
$$w_2 = \prod_k \tilde{a}^2(q_k - q_{k-1}),$$

with w_1 depending only on q_k's, and w_2 only on the increments of q_k's. These increments $q_k - q_{k-1} = \omega_k$ are supposed to be very small (as compared to $2E \geq 2m$), either because we have a really slow switching procedure with $w_i \lesssim \Delta$, and Δ small [case (a)], or because we are interested in approaching an essentially constant limit with $\omega_i \sim \Delta_n$, $\Delta_n \sim 1/n$ [case (b)]. We will also shrink the interaction number k axis by using a "time" variable

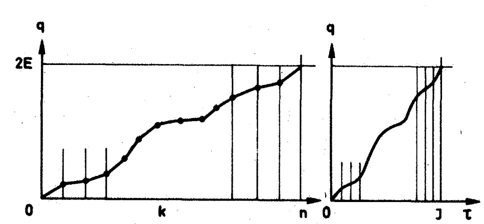

FIG. 2. The transition from a typical discrete path from $q(0) = 0$ to $q(n) = 2E$ in the q vs k plot to a continuous path in the q vs τ plot.

$$\tau = k\epsilon\,, \quad 0 \leqslant \tau \leqslant \mathcal{T}\,, \quad \mathcal{T} = n\epsilon\,. \tag{11}$$

In particular, we will choose

$$\Delta/\epsilon = \xi \text{ [case (a)]}, \quad \Delta_n/\epsilon_n = \xi \text{ [case (b)]}, \tag{12}$$

with ξ a constant of $O(1)$. For small ϵ and Δ the paths of Fig. 2 will be mapped into almost continuous trajectories with

$$q(\tau) = q(k) \tag{13}$$

and

$$\frac{dq}{d\tau} \equiv \dot{q}(\tau) = \frac{q_k - q_{k-1}}{\epsilon} = \frac{\omega_k}{\Delta}\frac{\Delta}{\epsilon} \equiv \alpha_k \xi \sim O(1)\,, \tag{14}$$

satisfying the boundary conditions

$$q(0) = 0\,, \quad q(\mathcal{T}) = 2E\,. \tag{15}$$

The transition to a continuous curve will be exact in the large-n limit of case (b), when the q and τ grid sizes Δ_n and ξ_n simultaneously go to zero. Writing the product [Eq. (10)] in exponential form we have

$$W_{\text{path}} = -\exp\left[\frac{1}{\epsilon}\left(\int_0^{\mathcal{T}} d\tau\,\{\ln[-g^2\tilde{a}^2(\epsilon\dot{q}(\tau))] - \ln[q(\tau)(2E - q(\tau))]\}\right)\right] \tag{16}$$

for each trajectory satisfying Eq. (15).

At this point it is very convenient to introduce a Lagrangian $L(q,\dot{q})$ in our fictitious energy space q, $L = T(\dot{q}) - V(q)$,

$$T(\dot{q}) = \ln[-g^2\tilde{a}^2(\epsilon\dot{q})]\,, \quad V(q) = \ln[q(2E - q)]\,. \tag{17}$$

The optimal stationary trajectory maximizing Eq. (16) or $\int_0^{\mathcal{T}} L(q,\dot{q})\,d\tau$ is then given by the Euler-Lagrange equation

$$\frac{d}{d\tau}\frac{dT(\dot{q})}{d\dot{q}} = -\frac{dV}{dq}\,. \tag{18}$$

Once $q(\tau)$ is known, $I = \int_0^{\mathcal{T}} L\,d\tau$ can be computed. Since L is not (explicitly) time dependent we have the energy integral

$$H = \dot{q}\,\frac{dT(\dot{q})}{d\dot{q}} - T(\dot{q}) + V(q) = c\,. \tag{19}$$

Thus we can write

$$\begin{aligned} I &= \int_0^{\mathcal{T}} d\tau[T(u) - V(q)] \\ &= \int_0^{\mathcal{T}} d\tau\left(u\frac{dT}{du} - c\right) \\ &= \underset{\text{(along trajectory)}}{\int_{u(0)}^{u(\mathcal{T})}} \frac{du}{u}\frac{dq}{du}[K(u) - c] \end{aligned} \tag{20}$$

with $u = \dot{q}$ and $K = u\,dT/du$.

Comparing T and V [Eq. (17)] to common mechanics problems, we notice an interesting inversion of the complexities of T and V. Rather than the simple $\dot{q}^2/2$, here we have a general kinetic term $T(\dot{q})$ related to the variety of slow perturbative interactions $a(t)$. However, we have a standard potential

$$V(q) = \ln[q(2E - q)]\,,$$

which reflects indeed the original purely kinematic propagators of the diagram. The explicit form of $V(q)$ allows us to express $q\ [= E \pm (E^2 - e^V)^{1/2}]$ and dq/du in terms of u, since V is given via energy conservation $V = c + T(u) - K(u)$ as a function of u. The (charge-conjugation) symmetry of the $q(\tau)$ curve with respect to $\tau = \mathcal{T}/2$, where in particular $q = E$, allows us to write the line integral [Eq. (20)] [which because of the symmetry $u(0) = u(\mathcal{T})$ describes a closed path] as twice the integral to the symmetry point $u^* = u(\mathcal{T}/2)$. As always in situations where boundary conditions $(q(0), q(\mathcal{T}))$ are given, rather than initial conditions $(q(0), \dot{q}(0))$ the determination of the energy has to be done via an implicit integral condition such as

$$\int_{q(0)}^{q(\mathcal{T})} \frac{d\tau}{dq}\,dq = \mathcal{T}\,. \tag{21}$$

Some of the more technical aspects associated with the determination of $u(0)$, u^*, and the energy constant c are dealt with in the Appendix.

Finally, let us notice that the inclusion of a linear term $-2gp_z\tilde{a}$ [and going over from Eq. (8) to Eq. (9) above] is fairly straightforward. We need only modify the kinetic part of the Lagrangian into

$$T(u) = \ln[g^2\tilde{a}^2(\epsilon\dot{q}(\tau)) - 2gp_z\tilde{a}(\epsilon\dot{q}(\tau))]\,. \tag{22}$$

IV. SOME SIMPLE APPROXIMATIONS AND EXAMPLES

To elucidate our general development it is instructive to consider some simple cases. The most drastic approximation to our analog mechanical problem[1] is to compute the trajectory by altogether neglecting the effect of the potential. We then have [cf. Eq. (19)] $\dot{q} = u = \text{const}$ and a simple straight-line trajectory

$$q(\tau) = 2E\tau/\mathcal{T}\,. \tag{23}$$

Coming back to our original discrete problem Eq. (8) [or (9)] this amounts to evaluating the integrand at the symmetry point $\omega_i = \bar{\omega} = 2E/n$. Clearly this is an extremum of the numerator function in Eq. (8) all by itself, since the numerator is a product of n identical functions with a symmetrical constraint $\delta(\sum_1^n \omega_i - 2E)$. We now evaluate the denominator (7) at the symmetry point

$$D^{(n)} \approx (-1)^{n-1}\left(\frac{2E}{e}\right)^{2n}\frac{1}{n}\,, \tag{24}$$

where we used Stirling's approximation (or, equivalently, integrated the potential $\ln[q(2E-q)]$ along the straight line (23) as is done in deriving this approximation). The integral of the numerator part of Eq. (8) by itself can be evaluated in many cases of interest. This is most conveniently done in Fourier transform (original t) space where

$$N=\int_{-\infty}^{\infty} dt\, e^{-2Eit}[g^2a^2(t)]^n\,. \tag{25}$$

For the case of a constant field $\mathcal{E}$, $a_c(t)=t\mathcal{E}$, and

$$N=\int_{-\infty}^{\infty} dt\, e^{-2iEt}(g^2t^2\mathcal{E}^2)^n$$
$$=\lim_{T\to\infty}\int_{-T}^{T} dt\, e^{-2iEt}(gt\mathcal{E})^{2n}\,. \tag{26}$$

As indicated, a switching procedure for the field is required so that it exists only over a finite domain $-T\leq t\leq T$. We can use

$$a(t)=t\mathcal{E}\theta(T+t)\theta(T-t)\,, \tag{27}$$

or some other more smooth θ-like function. In momentum space we have

$$\tilde{a}^2(\omega)=-\frac{d^2}{d\omega^2}\left(\frac{2\sin\omega T}{\omega}\right)\xrightarrow[T\to\infty]{}-\delta''(\omega)\,. \tag{28}$$

It should be noted that there are many ways of smearing the $\delta''(\omega)$ in ω space corresponding, e.g., to Lorentzian

$$\delta_\Delta(\omega)\approx\Delta/(\Delta^2+\omega^2)\,,$$

Gaussian

$$\delta_\Delta(\omega)\approx[(2\pi\Delta)^{1/2}]^{-1}\exp(-\omega^2/2\Delta^2)\,,$$

etc. δ-function versions. All of these can be treated by our general method. However, only the version of Eq. (28) corresponds to a time profile with really constant field.

Returning to Eqs. (26) and (24) we have for $E^2\gg g\mathcal{E}$

$$A=\sum_n A_n=-\sum_{n=1}^{\infty}\int_{-T}^{T} dt\, e^{-2iEt}n\left(\frac{2E}{e}\right)^2\left[\frac{-g^2\mathcal{E}^2t^2}{(2E/e)^2}\right]^n\sim\int_{-T}^{T}dt\frac{e^{-2Eti}E^2[g\mathcal{E}t/(2E/e)]^2}{\{1+[tg\mathcal{E}/(2E/e)]^2\}^2}\sim\frac{E^5}{(g\mathcal{E})^2}\exp\left(-\frac{4E^2}{eg\mathcal{E}}\right). \tag{29}$$

The pair-production rate will then be proportional to

$$\int\frac{d^3p}{2E}|A|^2\sim\int\frac{d^3p}{E}\frac{E^{10}}{(g\mathcal{E})^4}\exp\left(-\frac{8E^2}{eg\mathcal{E}}\right)\sim\exp\left(-\frac{8m^2}{eg\mathcal{E}}\right), \tag{30}$$

since the lower limit of $E(\vec{p})$ is $E(0)=m$. [For simplicity, we assumed that Eq. (29) applies also to $p_z\neq0$, an issue which will be taken up shortly.] We observe that Eq. (30) has the correct functional behavior of the leading term in the exact formula, Eq. (1). The straight-line approximation to the action integral amounts to replacing the π in the exponential of Eq. (1) by $8/e$ in Eq. (30) which is roughly 10% accurate. Equation (29) involves some delicate point of interchanging summation, integration, and the $T\to\infty$ limit. In fact, the various A_n's behave like

$$A_n\sim(2n)!\,c^{2n}\,, \tag{31}$$

and picking the complex-pole residue in the t plane [Eq. (29)] constitutes a Borel-type ansatz for the summation over n. For a simple asymptotic estimate of A_n let us return to the $\omega_i=\bar{\omega}=2E/n$ approximation and apply it to the numerator of Eq. (8) as well. For variety (and simplicity) let us consider instead of $\tilde{a}^2(\omega)$ of Eq. (28),

$$\tilde{a}^2(\omega)=-\delta_\Delta''^{\text{Gaussian}}(\omega)=\frac{-1}{\sqrt{2\pi}\,\Delta^3}\exp\left(-\frac{\omega^2}{2\Delta^2}\right)\left(1-\frac{\omega^2}{\Delta^2}\right). \tag{32}$$

We then have

$$A_n\sim\frac{N_n}{D_n}\bigg|_{\{\omega_i=\bar{\omega}\}}\int d\omega_1\cdots d\omega_n\delta\left(2E-\sum_i\omega_i\right)=[a\bar{\alpha}^3(1-\bar{\alpha}^2)\exp(-\tfrac{1}{2}\bar{\alpha}^2)]^n\left(\frac{g\mathcal{E}}{E^2}\right)^{2n}(2n)!\,, \tag{33}$$

with $\bar{\alpha}=\bar{\omega}/\Delta=2E/n\Delta$ and a is a numerical constant. The important points, which should be noted, are the following:

(i) The expression in square brackets attains its maximum at $\bar{\alpha}=(3+\sqrt{6})^{1/2}\approx2.3$, which is n independent so that $A_n\sim C^n 2n!$. We also find that the width Δ_n introduced should be smaller for larger n,

$$\Delta \to \Delta_n \sim \frac{1}{\xi}\frac{2E}{n}\,. \tag{34}$$

As mentioned already in the Introduction, this is appropriate for the case at hand [case (b)] where the smearing Δ_n is just a theoretical device and not controlled by any experimental setup. Only by using an increasingly finer mesh can we make the estimate of the high terms in the series asymptotically exact and thus capture the singular tunneling behavior.

(ii) The value $\bar{\alpha}$ is larger than 1, i.e., $\bar{\alpha}$ occurs to the right of α_0, the location of the first zero in $\tilde{a}^2(\omega)$, so $\tilde{a}^2$ is positive there, and there are no sign oscillations between the contributions of successive A_n [examples of $\tilde{a}^2$ are discussed in the Appendix after Eq. (A2)]. In the Appendix we shall show that a larger-n behavior of (31) can be obtained under quite general considerations.

Finally we can try to see the effect of the linear (p_z) term in this case. This amounts, in this case, to the replacement

$$g^2\mathcal{E}^2\delta''_\Delta(\omega) \to g^2\mathcal{E}^2\delta''_\Delta(\omega) + 2ig\mathcal{E}p_z\delta'_\Delta(\omega)\,,$$

which, at the symmetry point, simply modifies the result of Eq. (33) by

$$\left[1+\frac{2ip_zE}{ng\mathcal{E}(\bar{\alpha}^2-1)}\right]^n \to \exp\left[\frac{2ip_zE}{g\mathcal{E}(\bar{\alpha}^2-1)}\right], \tag{35}$$

i.e., to a common phase factor which is clearly irrelevant for the asymptotic part of the series, the part responsible for tunneling. The transverse-momentum spectrum of Ref. 3

$$d\sigma/dp_T{}^2 \sim \exp\left(-\frac{\pi}{g\mathcal{E}}p_T{}^2\right)$$

can therefore be generalized to

$$\frac{d^3\sigma}{dp^3} \sim \exp[-\pi(p_T{}^2+p_z{}^2)/g\mathcal{E}]\,. \tag{36}$$

V. SUMMARY AND CONCLUSIONS

In this work we have addressed the question of pair creation in slowly varying or essentially constant electric field, using Feynman diagrams in momentum space. Rather than attempt a direct exact evaluation of finite-order diagrams we observed that in very large orders n of perturbation, which are essentially forced upon us by the boundary conditions of the problem, a considerable simplification arises. In fact, we can mimic in momentum space the classical tunneling process by following the increase of energy of the pair as they are accelerated by the field via the absorption of many soft photons. Feynman diagrams reduce in this limit to path integrals in momentum space and the dominant path can be found via the classical Hamilton principle and the Euler-Lagrange equation. The final result has certain similarity to the large-order behavior in field theory[4] found via essentially a similar method, except that classical solutions in configuration space have been investigated.

It has been suggested on many occasions that classical solutions (or dual amplitudes) may arise by considering dense Feynman diagrams. It is conceivable that the quark-duality diagram model should be considered as planar QCD diagrams which are dense in momentum space—with only the quarks being allowed finite changes of their momenta via interaction with (or rather exchange of) many soft gluons. Such a case has some analogy to the case considered here. Our approach might therefore be useful in its study.

ACKNOWLEDGMENTS

We thank our colleagues in the theory group of the Max-Planck-Institute for Physics for discussions. The work of C. B. Chiu was supported in part by the Alexander von Humboldt Foundation.

APPENDIX: MORE DETAILS ON THE ACTION INTEGRAL

In this appendix we consider in some detail the evaluation of the action integral along the classical trajectory. Technically speaking we should confine ourselves to the general case where the classical trajectory q is a monotonic function of τ (i.e., $\dot{q}>0$ or $\alpha>0$). We shall refer to this as the monotonicity ansatz. No explicit restriction on the sign of $\ddot{q}$ (or $\dot{\alpha}$) is needed below.

First consider the initial conditions of the classical trajectory. Since the differential of q is involved in specifying initial conditions, $q(0)$, $\dot{q}(0)$ (or α_1), we shall evaluate them immediately after the first step, i.e., at $k=1$ or $\tau=1/n$. Denote

$$T(\dot{q}) = \ln(g^2 f/\Delta^3) \equiv \ln(g^2/\Delta^3) + T'\,,$$

$$V(q) = \ln\left[(2E)^2\frac{q}{2E}\left(1-\frac{q}{2E}\right)\right] = \ln(2E)^2 + V'\,,$$

and the reduced Hamiltonian $H'=V'+T'=c'$.

From Eqs. (17) and (19) we get

$$e^{V'} \equiv fe^{c'}e^{-\alpha f_\alpha/f} = \frac{q}{2E}\left(1-\frac{q}{2E}\right), \quad \text{with } f_\alpha = \frac{df}{d\alpha}\,. \tag{A1}$$

The monotonicity ansatz requires $f>0$. At this point $q=\omega$, so $q/2E=\alpha/\xi n$. For very large N, we have

$$fe^{c'-\alpha f_\alpha/f} \approx \frac{\alpha}{\xi n} \ll 1\,. \tag{A2}$$

Before proceeding to solve for α, we first discuss briefly the profile function f, which we recall is a function of α only, its behavior dependent upon the switching-on and -off procedure assumed. To extract the general features of f we shall use the step-function cutoff and the Gaussian cutoff as a guide. The qualitative common features of these two profiles are shown in Fig. 3, in particular $f(0)<0$. The first simple zero occurs at $\alpha=\alpha_0$, which is of the order of unity. Beyond this point f rises to a maximum and then falls. As α further increases, f may or may not have further oscillations. We shall not be concerned with this large-α behavior.

Substituting (A2) into (A1) for large n one gets an initial value of α to occur at

$$\alpha_1\approx\alpha_0\left[1+\frac{1}{\ln(\xi e^{c'}f_{\alpha_0})+\ln(n/\ln n)}\right]. \tag{A3}$$

In terms of the q variables, our initial conditions are

$$q\approx\frac{2E\alpha_0}{\xi n}\quad\text{and}\quad\dot q\approx\frac{2E\alpha_1}{\xi}. \tag{A4}$$

A glance at (A3) reveals that the initial velocity, depends on the energy constant c', which has already been alluded to the text, and is implicitly given via the relation

$$\tfrac12\mathcal{T}=\int_0^{\mathcal{T}/2}d\tau=\frac{1}{\xi}\int_{\alpha_1}^{\alpha^*}\frac{d\alpha}{\alpha}\frac{dq}{d\alpha}, \tag{A5}$$

where α^* is the velocity at the symmetry point. Here α^* satisfies

$$e^{c'}fe^{-\alpha f_\alpha/f}\big|_{\alpha=\alpha^*}=\tfrac14. \tag{A6}$$

The derivative $dq/d\alpha$ in (A5) may be obtained from (A1) together with the condition that the initial point is at $\alpha=\alpha_1$, $dq/d\alpha>0$, as implied by the monotonicity ansatz. In particular,

$$\frac{dq}{d\alpha}=2E\frac{\alpha\xi}{f}(f_{\alpha\alpha}-f_\alpha{}^2)\frac{e^{V'}}{(1-4e^{V'})^{1/2}},\quad\text{where } f_{\alpha\alpha}=\frac{d^2f}{d\alpha^2}, \tag{A7}$$

with $\xi=\operatorname{sign}(f_{\alpha\alpha}-f_\alpha{}^2)_{\alpha_1}$. Now Eq. (A5), together with (A6) and (A7) specifies completely the transcendental equation for the determination of α^*.

Finally, the reduced action evaluated along the classical path is

$$\begin{aligned}I_c'&\equiv\int_0^{\mathcal{T}}d\tau\,\frac{1}{\mathcal{T}}\left(\frac{\alpha f_\alpha}{f}-c'\right)\\&=2\int_{\alpha_1}^{\alpha^*}d\alpha\,\frac{\alpha f_\alpha}{f^2}\xi(f_{\alpha\alpha}-f_\alpha{}^2)\frac{e^{V'}}{(1-4e^{V'})^{1/2}}-c'.\end{aligned} \tag{A8}$$

The important point to note here is that I_c' is independent of n.

To exhibit explicitly the normalization involved, let us backtrack one step. For large n, the nth-order amplitude of Eq. (8) is now given by

$$\begin{aligned}A_n&\sim\left(\frac{g\mathcal{E}}{2E\Delta}\right)^{2n}\int d\alpha_1\cdots d\alpha_n\delta\Big(n\bar\alpha-\sum\alpha_i\Big)e^{nI'}\sim\left(\frac{g\mathcal{E}e^{I_c'/2}}{2E\Delta}\right)^{2n}\int_{\text{KE cutoff}}d\alpha_1\cdots d\alpha_n\delta\Big(n\bar\alpha-\sum_i\alpha_i\Big)\\&\sim\left(\frac{g\mathcal{E}}{E^2}\right)^{2n}\left[\frac{\xi}{8}\exp(1+I_c'/2)\right]^{2n}2n!\int_{\text{KE cutoff}}d\alpha_1\cdots d\alpha_n\delta\Big(n\bar\alpha-\sum_i\alpha_i\Big).\end{aligned} \tag{A9}$$

In the second step we have explicitly factored out the term involving the action integral evaluated along the classical trajectory. As usual in the evaluation of the multiplicative normalization factor associated with the spread around the classical trajectory, strong damping is expected to come from the kinetic term. This is indicated by the label "KE cutoff." Using Eq. (34) for the definition of the quantity Δ and the Stirling approximation which converts the most dominant large-n dependence into the vectorial form, one arrives at the last expression. This is an asymptotic expression for large n. Notice that the multiplica-

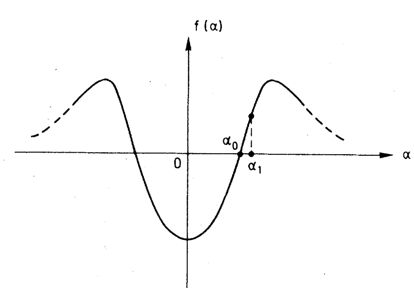

FIG. 3. An illustration of the function $f(\alpha)$, where α_0 denotes the α value of the first zero and α_1 the initial value of α.

tive factor outside of the integral has the large-n dependence precisely of the form of Eq. (31). One expects that the dominant large-n dependence of the integral is at most of the power form: $(\text{const})^n$. This can easily be checked at least for the two extremes, where one either ignores the kinetic cutoff effect or the δ-function constraint. Since the inclusion of the extra power term is still compatible with Eq. (31), we see that the asymptotic behavior specified by Eq. (31) is indeed general, although the specific coefficient of the power is more sensitive to the approximations involved.

---

*Permanent address: University of Texas, Austin, Tex. 78712.

†Permanent address: Physics Department, Tel-Aviv University, Ramat-Aviv, Tel-Aviv, Israel.

[1]W. Heisenberg and H. Euler, Z. Phys. 38, 714 (1938); V. S. Weisskopf, K. Dan. Vidensk. Selsk, Mat.-Fys. Medd. 14, No. 6 (1936); J. Schwinger, Phys. Rev. 82, 664 (1951); 93, 615 (1954).

[2]E. Brezin and C. Itzykson, Phys. Rev. D 2, 1191 (1970).

[3]A. Casher, H. Neuberger, and S. Nussinov, Tel-Aviv University report, 1978 (unpublished).

[4]L. N. Lipatov, Zh. Eksp. Teor. Fiz. Pis'ma Red. 24, 179 (1976) [JETP Lett. 24, 157 (1976)]; Zh. Eksp. Teor. Fiz. 72, 411 (1977) [Sov. Phys.-JETP 45, 216 (1977)]. C. Itzykson, G. Parisi, and J. B. Zuber, Phys. Rev. D 16, 996 (1977); G. Parisi, Phys. Lett. 66B, 167 (1977).

[5]S. Chadha and P. Olesen, Phys. Lett. 72B, 87 (1977).